Multi-patch B-Spline Statistical Shape Models for CAD-Compatible Digital Human Modeling

Huysmans, Toon; Danckaers, Femke ; Vleugels, Jochen ; Lacko, Daniël ; De Bruyne, Guido; Verwulgen, Stijn; Sijbers, Jan

DOI
10.1007/978-3-319-94223-0_17

Publication date
2019

Document Version
Final published version

Published in
Advances in Human Factors in Simulation and Modeling

Citation (APA)
Huysmans, T., Danckaers, F., Vleugels, J., Lacko, D., De Bruyne, G., Verwulgen, S., & Sijbers, J. (2019). Multi-patch B-Spline Statistical Shape Models for CAD-Compatible Digital Human Modeling. In D. N. Cassenti (Ed.), *Advances in Human Factors in Simulation and Modeling : Proceedings of the AHFE 2018 International Conferences on Human Factors and Simulation and Digital Human Modeling and Applied Optimization* (pp. 179-189). (Advances in Intelligent Systems and Computing; Vol. 780). Springer. https://doi.org/10.1007/978-3-319-94223-0_17

Multi-patch B-Spline Statistical Shape Models for CAD-Compatible Digital Human Modeling

Toon Huysmans[1,2(✉)], Femke Danckaers[2], Jochen Vleugels[3], Daniël Lacko[3], Guido De Bruyne[3], Stijn Verwulgen[3], and Jan Sijbers[2]

[1] Section on Applied Ergonomics and Design, Faculty of Industrial Design Engineering, Delft University of Technology, Delft, The Netherlands
t.huysmans@tudelft.nl
[2] imec - Vision Lab, Department of Physics, Faculty of Science, University of Antwerp, Antwerp, Belgium
[3] Department of Product Development, Faculty of Design Sciences, University of Antwerp, Antwerp, Belgium

Abstract. Parametric 3D human body models are valuable tools for ergonomic product design and statistical shape modelling (SSM) is a powerful technique to build realistic body models from a database of 3D scans. Like the underlying 3D scans, body models built from SSMs are typically represented with triangle meshes. Unfortunately, triangle meshes are not well supported by CAD software where spline geometry dominates. Therefore, we propose a methodology to convert databases of pre-corresponded triangle meshes into multi-patch B-spline SSMs. An evaluation on four 3D scan databases shows that our method is able to generate accurate and water-tight models while preserving inter-subject correspondences by construction. In addition, we demonstrate that such SSMs can be used to generate design manikins which can be readily used in SolidWorks for designing well conforming product parts.

Keywords: Statistical shape modeling · B-splines · Computer-aided design
Digital human modeling

1 Introduction

In user-centered product design, ergonomics is pursued by putting the physical and mental characteristics of the human user center-stage [1]. For products that are worn on the body or closely interact with it, e.g. wearables, garments, seating furniture, etc., 'body shape' is a dominant physical characteristic with an impact on product affordance, comfort, and wearability [2]. Statistical shape models (SSM) are an elegant way to represent body shape variation observed in a population. SSMs typically represent shape variation by a shape space with the average shape at the origin and spanned by a small set of orthogonal shape modes. In this way, each point in the shape space represents a specific body shape and its coordinates define the contribution/weight of each shape mode. In this formulation, the weights are *body shape parameters* and such parametric body models are considered a valuable tool for user-centered product design [3].

A large part of the research on statistical shape modeling is devoted to methodologies for the construction of inter-subject correspondences and mathematical

D. N. Cassenti (Ed.): AHFE 2018, AISC 780, pp. 179–189, 2019.
https://doi.org/10.1007/978-3-319-94223-0_17

formulations of the statistical model that is derived from these correspondences. Many algorithms are available from the literature, both for organ modeling [4–6], mostly within the medical imaging field, as well as for full body modeling [7–12]. Most of these works construct SSMs from 3D triangle meshes, obtained from 3D scanning or medical imaging. Naturally, the derived SSM is also represented in triangular mesh form. Other geometric representations for SSMs are available, e.g. landmarks, medial models, level-sets, or basis-functions [4], but they are much less widespread.

For user-centered design, the predominance of triangular mesh SSMs is somewhat unfortunate since digital models in the form of triangular meshes are not well supported by popular CAD packages (e.g. SolidWorks). There, the majority of CAD operations is only available for B-spline geometry and while reverse engineering allows the conversion of triangular geometry to B-splines, for organic shapes it is often a slow and cumbersome process. In addition, it generally results in a varying number and distribution of patches, even for shapes generated by the same SSM. As a result, inter-subject correspondences are lost and, with it, the ability to consistently link (parametric) designs to anatomical reference points on these shapes. SSMs with a spline-based representation could improve compatibility of SSMs with CAD-software.

Only limited work has been done on spline based SSMs. In [13], Quan et al. built a B-spline SSM of the face. They took as input triangular meshes with a pre-existing vertex correspondence, then parameterized the meshes using cylindrical coordinates and subsequently fitted the scans with a single B-spline patch. Unfortunately, the cylindrical mapping approach only handles simple geometries with disc-like topology. Hu et al. constructed SSMs of organs in the pelvic area using a NURBS representation and deformation [14]. The NURBS, however, was manually constructed using the loft tool in Rhinoceros and their NURBS deformation technique was only demonstrated on very coarse organ approximations. From the brief description of the method it is unclear whether the method can be applied to more detailed and/or complex shapes. In [15], Peng et al. employed conformal mapping to obtain a T-spline SSM of the face and its expressions. Similar to [13], their method is developed for shapes of disc topology and further modification would be required to apply the methodology to more complex shapes.

In this paper, an automated methodology is proposed that allows the construction of SSMs with a B-spline representation with less restrictions on topology or shape. Our method takes as input a set of pre-corresponded triangular meshes and generates as output a multi-patch B-spline SSM, where the B-spline patch topology is derived from a rough quadrilateral mesh approximation of the mean shape of the triangular SSM. Shape instances generated by our B-spline SSMs have consistent patch layout and seamlessly integrate with parametric CAD-software, where they can be utilized for ergonomic product design.

2 Methods

Starting from a set of triangular meshes (the population sample), with a one-to-one vertex correspondence, our method constructs an SSM with a B-spline representation in three phases. The process is visualized in Fig. 1.

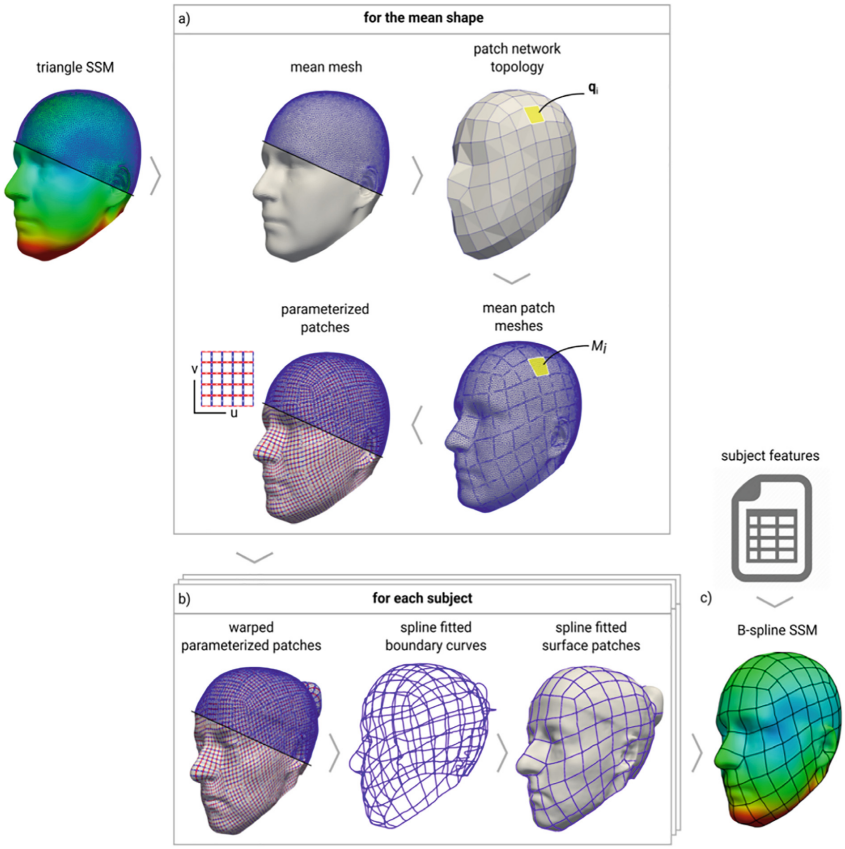

Fig. 1. A depiction of the steps of our method for the construction of a B-spline statistical shape model. See text for the explanation of the different steps.

In the first stage (Fig. 1a), the B-spline patch network topology for our SSM is defined, based on a rough quadrangulation of the mean shape. The mesh of the mean shape is then split into smaller patches, one patch per quad in the quadrangulation, and the vertices of the patches are equipped with uv-parameters, using a convex combination mapping, to facilitate B-spline fitting. In the second stage (Fig. 1b), the shape of each subject is approximated with a multi-patch B-spline surface. The approximation is achieved by first warping the modified mean mesh to the subject's shape via the vertex correspondence, followed by a B-spline curve approximation of the patch boundaries, and finally by a B-spline surface approximation for each of the patches where the approximation interpolates the B-spline patch boundary curves to ensure watertightness of the surface. In the final stage (Fig. 1c), the SSM is calculated from the B-spline approximations by applying principal component analysis (PCA) to the control point coordinates and a further parametric body model can be derived via a regression analysis of the 3D shapes versus subject features.

In the following sections, a more elaborate description of the involved steps is provided.

2.1 Patch Layout

Our method starts from a set of n_s shapes $S = \{S_1, \ldots, S_{n_s}\}$ in triangular mesh form with a pre-existing vertex correspondence. Thus, each shape S_i is described by a set of n_v vertices $\left\{\boldsymbol{v}_1^i, \ldots, \boldsymbol{v}_{n_v}^i\right\}$, with $\boldsymbol{v}_j^i \in \mathbb{R}^3$ at the same anatomical location for each i. The surfaces S_i all share the same mesh connectivity consisting of n_t triangles. From these surfaces, the mean shape M can be derived with n_v vertices $\{m_1, \ldots, m_{n_v}\}$ and $m_i = \frac{1}{n_s}\sum_{j=1}^{n_s} \boldsymbol{v}_i^j$. The mean shape M is fairly smooth but still contains the common characteristic features of the shapes under consideration. We therefore consider it as a good starting point to define the B-spline patch layout for our SSM. The patch layout is obtained by approximating M with a rough quadrangular (or quad) mesh Q using the mixed-integer quadrangulation method of Bommes et al. [17]. Any other method that generates a conforming quadrangulation, i.e. without T-junctions, could be used equally well [16]. The obtained quad mesh is described by a set of $n_p \ll n_v$ vertices in $\mathbb{R}^3$ and a set of $n_q \ll n_t$ quads. The connectivity of this quad mesh Q will be used to define the connectivity of the B-spline patches of the SSM in the next steps. There will be one patch per quad and the neighborhood relation of the quads will be adopted for the patches.

The mean mesh M is split into a set of smaller meshes, one mesh for each quad. Let us consider a quad q from Q with vertices (c_1, c_2, c_3, c_4). First, each of the four corners c_i is mapped to the closest vertex on M, denoted r_i. Here, the closest point search for points that are on the boundary of Q is limited to the boundary vertices of M. Then, for each edge $e = (c_k, c_l)$ of the quad, a geodesic curve g between the corresponding vertices (r_k, r_l) on M is traced using the method of Kimmel and Sethian [18]. Finally, by cutting the mesh M along the four obtained geodesic curves, the surface patch that corresponds to quad q can be extracted. This procedure is executed for each quad q_i in Q, resulting in the split of mean mesh M into a set of n_q patches $\left\{M_1, \ldots, M_{n_q}\right\}$. The i-th patch M_i is described with n_i vertices m_j^i, either directly inherited from M or introduced by the cutting of triangles along the geodesic paths.

Each of the meshes M_i will contribute one B-spline patch to the SSM. In order to facilitate B-spline approximations in the next phase of our methodology, the vertices m_j^i of mesh patches M_i are equipped with uv-coordinates $u_j^i \in [0,1]\times[0,1]$, defining their location in the parameter space of the B-spline. First, the perimeter of M_i is mapped to the perimeter of the parameter space. The four corner points of M_i, corresponding to the quad corners of q_i, are mapped to the four corners of the rectangular B-spline parameter space. The four boundary segments of M_i, connecting the patch corners, are mapped to the straight boundary segments of the parameter space using arc-length parameterization. The mapping of the boundary of M_i is extended to the interior vertices of M_i via the mean value surface parameterization method of Floater [19, 20]. This guarantees a one-to-one map between the surface of M_i and the B-spline parameter space, resulting in a complete and unambiguous parameterization of the patch for fitting. In addition, for neighboring patches, the parameterization of common boundary curves matches up,

which is a requirement in our methodology in order to ensure water-tightness of the B-spline SSM.

2.2 B-Spline Approximation

For each shape S_i in the population, a multi-patch B-spline approximation is calculated based on the parameterized patches obtained in the previous step. First, the vertices of all the surface patches M_j are warped to match the shape of S_i and will be denoted M_j^i. For vertices on M_j inherited from M, this warping is trivially derived from the vertex correspondence between M and S_i. Vertices of M_j that were newly introduced during the splitting of M into patches, however, do not have an explicit correspondence with M or S_i. For these vertices, the warping is derived by barycentric interpolation with respect to the triangle of M in which the vertex was inserted.

The actual B-spline approximation of S_i, via the warped patches M_j^i, is obtained in two steps, in order to ensure water-tightness. First, the boundary segments of the warped patches are approximated with 3D uniform cubic B-spline curves, exactly interpolating the patch corners. This is followed by the approximation of each patch with a 3D uniform bi-cubic B-spline surface, exactly interpolating the previously calculated B-spline boundary curves. Robustness with respect to overfitting and undersampling is guaranteed by Tikhonov regularization promoting patch smoothness.

In this procedure, B-spline curves are specified by a set of n_k uniformly spaced knots $K = \{k_i\}$ in $\mathbb{R}$ and n_k control points $P = \{p_i\}$ in $\mathbb{R}^3$. The B-spline curve t, parameterized by a 1D parameter u, is then defined as

$$t(u|K,P) = \sum_{i=1}^{n_k} \beta_{i,4}(u) p_i, \tag{1}$$

where $\beta_{i,4}$ is the i-th 1D cubic B-spline kernel [21] corresponding to the knot sequence $\{k_1, k_1, k_1, k_1, k_2, \ldots, k_{n_k-1}, k_{n_k}, k_{n_k}, k_{n_k}, k_{n_k}\}$.

Similarly, B-spline surface patches are specified by a set of $n_k \times n_k$ knots $K = \{k_{ij}\}$ in $\mathbb{R}^2$ with uniform spacing and $n_k \times n_k$ control points $P = \{p_{ij}\}$ in $\mathbb{R}^3$. The B-spline surface s is parameterized by the 2D parameter $u = (u, v)$ and is defined as

$$s(u|K,P) = \sum_{i=1}^{n_k} \sum_{j=1}^{n_k} \beta_{i,4}(u) \beta_{j,4}(v) p_{ij}. \tag{2}$$

For a given patch boundary curve with n_c points $\boldsymbol{x}_i$ and parameters u_i, the approximation with a B-spline curve $\boldsymbol{c}$ entails finding the optimal control points $\hat{P}$ and is formulated as the following minimization problem:

$$\begin{aligned} \hat{P} = \arg\min_P \|BP - X\|^2 + \tau LP^2, \\ \text{subject to } CP = D. \end{aligned} \tag{3}$$

The first term of the minimization objective measures the distance between the points x_i and the B-spline point $t(u_i)$, i.e. the fit of the curve. The $n_c \times 3$ matrix X contains the stacked boundary points x_i and the $n_k \times 3$ matrix P is formed by stacking the unknown control points. In the sparse $n_c \times n_k$ matrix B, the i-th row contains for each control point p_j the weight $\beta_{j,4}(u)$ it contributes to the B-spline point $t(u_i)$. The second term measures the smoothness of the B-spline curve, weighted by a factor τ, by means of summing the discrete Laplacian at each interior control point p_j. This Laplacian operator is formed by the rows of the sparse $(n_k - 2) \times n_k$ matrix L as

$$L_{ij} = \begin{cases} 2, & i = j \\ -1, & |i - j| = 1 \\ 0, & otherwise \end{cases}. \tag{4}$$

The equality constraint enforces the fixation of the two curve end-points at the patch boundary end-points. The $2 \times n_k$ matrix C is sparse and has a 1 on the first row at the index of the first control point and on the second row at the index of last control point. The 2×3 matrix D contains the stacked start and end point of the patch boundary. The minimum of Eq. (3) is obtained by solving the normal equations $(B^T B + \lambda L^T L)P = B^T X$ using a sparse LU factorization [22] with Karush-Kuhn-Tucker conditions to enforce the equality constraints.

For the fitting of the surface patches an analogous procedure as in Eq. (3) is followed. Matrix X is formed as before by stacking the patch points, P contains the grid of unknown control points in row-major order, and matrix B now contains the row-major ordered weights $\beta_{i,4}(u)\beta_{j,4}(v)$ for the grid of control points p_{ij}. The matrix L computes the 2D discrete Laplacian, with a central weight of 4 and a weight of -1 for the four incident control points on the grid. Finally, the equality constraints simply match the control points at the boundaries $u = 0$, $v = 1$, $u = 1$, and $v = 0$ with the control points of the previously calculated boundary B-spline curves. The resulting sparse system is again solved with LU-factorization.

The approach outlined in this section results in a water-tight, multi-patch approximation of each subject preserving the inter-subject correspondences.

2.3 SSM Construction

In order to calculate a B-spline SSM, each subject is represented by a n-dimensional vector obtained by concatenating the coordinates of all control points of all its B-spline patches calculated in the previous section. By applying a PCA on the resulting n_s vectors of dimension n a linear model of the variation is obtained:

$$\Theta = \bar{\Theta} + \sum_{i=1}^{n_s - 1} w_i \ddot{\Theta}_i. \tag{5}$$

Here, Θ is the nD vector of control point coordinates of the modeled shape, $\bar{\Theta}$ is the n D vector of mean control point coordinates, $\ddot{\Theta}_i$ are the $n_s - 1$ principal component vectors of dimension n providing a basis for the space of shape variations, and the

weights w_i control the contributions of the shape variations for a specific shape Θ. Typically, the weights w_i are allowed to vary in the range $|w_i| < 3\sqrt{\lambda_i}$, where λ_i is the i-th eigenvalue obtained in the PCA. In order to reconstruct the B-spline patches of the modeled shape, the control points of each patch in Θ are inserted in Eq. (2).

Following the approach of Allen et al. [7], a further body model is constructed that is parameterized by subject features, such as height, age, BMI, etc. The parameterization is captured by an $(n_s - 1) \times (n_f + 1)$ linear mapping matrix Π that maps subject features f_j onto the PCA weights $\mathrm{w}_i = [w_1 \ldots w_{n_s-1}]^T$ for each subject:

$$\Pi[f_1 \ldots f_{n_f} 1]^T = \mathrm{w}_i. \tag{6}$$

The mapping matrix is obtained by solving $\Pi = WF^+$, where W is the $(n_s - 1) \times n_s$ matrix of stacked subject PCA weights w_i, F is the $(n_f + 1) \times n_s$ matrix of stacked subject feature vectors, and F^+ denotes the pseudo-inverse of F. With the obtained mapping matrix Π, Eq. (5) can be rewritten to obtain a model parameterized by subject features:

$$\Theta(f_1, \ldots, f_{n_f}) = \bar{\Theta} + \ddot{\Theta}\Pi[f_1 \ldots f_{n_f} 1]^T, \tag{7}$$

where $\ddot{\Theta}_i$ is the $n \times (n_s - 1)$ matrix obtained by horizontally stacking the $n_s - 1$ principal components $\ddot{\Theta}_i$.

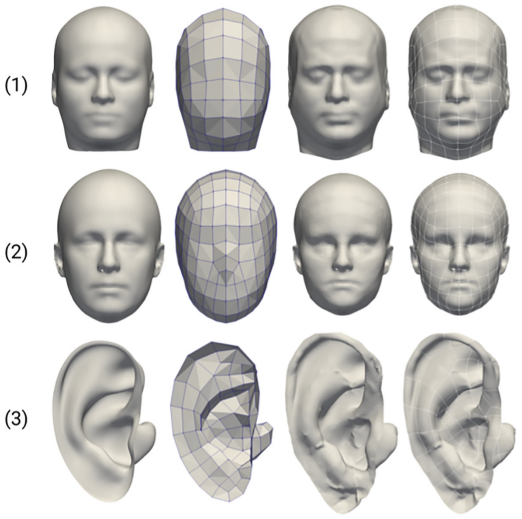

	# patches	# knots	τ
(1)	95	8x8	0.01
(2)	139	12x12	0.01
(3)	112	12x12	0.01
(4)	200	10x10	0.01

Fig. 2. The four datasets the methodology was evaluated on: (1) MRI heads, (2) CAESAR heads, (3) ear molds, and (4) femurs. For each dataset, from left to right, the mean shape, the quad mesh, a population subject, and the B-spline fit of that subject as calculated by our method. The table lists the chosen parameters that are required as inputs to our methodology.

2.4 SolidWorks AddIn

The authors developed a custom SolidWorks AddIn that allows the creation of instances of the parametric body models as native (B-spline) surfaces in SolidWorks. The AddIn with GUI was written in VB.net. The AddIn communicates with a custom written C#-library that encapsulates the model IO (HDF5 format) and shape generation process of Eq. (6).

3 Results

Our methodology was applied to four datasets: (1) 100 head surfaces, 50 male and 50 female subjects, extracted from MRI data in the ICBM database [23], (2) 1384 head surfaces from the CAESAR laser scan database [24], comprising 346 surfaces each of the groups male-Dutch, female-Dutch, male-Italian, and female-Italian, (3) 150 ear scans based on laser scans of silicone ear molds, and (4) 189 femur surfaces extracted from CT scanning. All surfaces were triangle meshes and inter-subject correspondences were calculated with previously published methods of the authors: the elastic surface registration method of [25] for datasets (1) and (2) and the cylindrical correspondence method of [6] for datasets (3) and (4). Intermediate results for each of the four datasets are shown in Fig. 2, along with the input parameters required by our methodology.

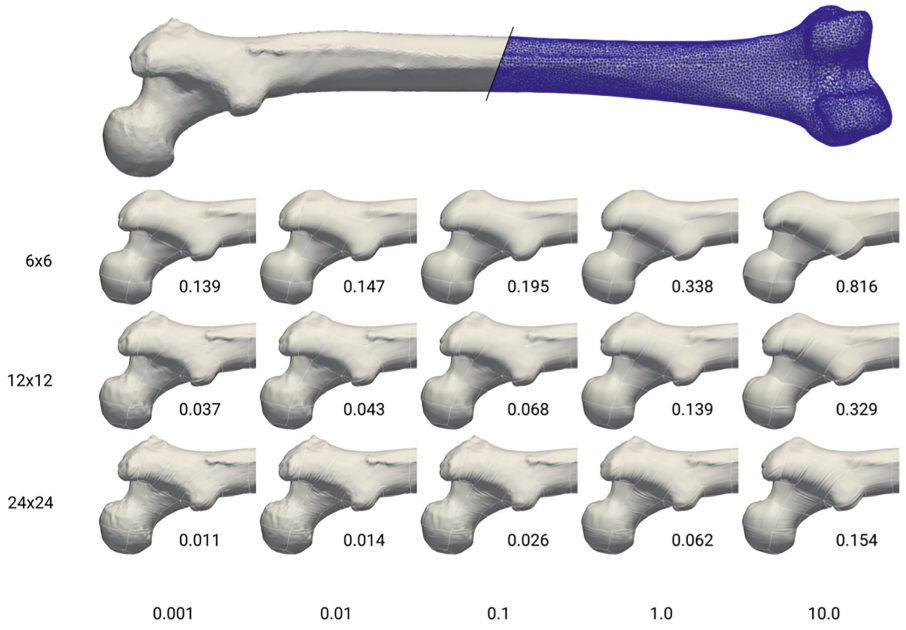

Fig. 3. Top: the triangle mesh of the first subject in the femur dataset. Bottom: resulting B-spline fits of this subject with varying number of control points per patch (rows) and Tikhonov regularization factors τ (columns). The fitting error is also provided for each case, measured as RMS surface distance from the mesh to the B-spline fit (in mm).

An experiment was performed on the femur dataset to investigate the influence of the number of control points per patch and the Tikhonov regularization factor τ (cfr. Eq. (3)) on the B-spline fitting. A multi-patch B-spline fit was calculated for the first subject of the database with combinations of, on the one hand, grids of 6×6, 12×12, and 24×24 control points per patch, and on the other hand, Tikhonov regularization factors of 0.001, 0.01, 0.1, 1.0, and 10.0. The resulting B-spline surfaces are shown in Fig. 3. There, also an estimate of the surface fit is provided by means of the root mean square (RMS) surface distance, measured from the triangle mesh vertices to the closest points on the B-spline surface.

The most computationally intensive part of our methodology is the fitting of the B-spline patches for all subjects in the population. For all datasets, the computation time per subject took up to 2s on a single core of an i7-5960X CPU.

In order to demonstrate our SolidWorks AddIn, a parametric model, with a variety of subject features such as 'head length' and 'head width', was calculated from the MRI head dataset and loaded into SolidWorks via our AddIn. Four head shapes (manikins) were generated: the average head and three heads with varying head width (percentile 5, 50 and 95). Finally, the average head manikin was employed to construct a part with perfect fit to the body using standard SolidWorks CAD-operations. The results are shown in Fig. 4.

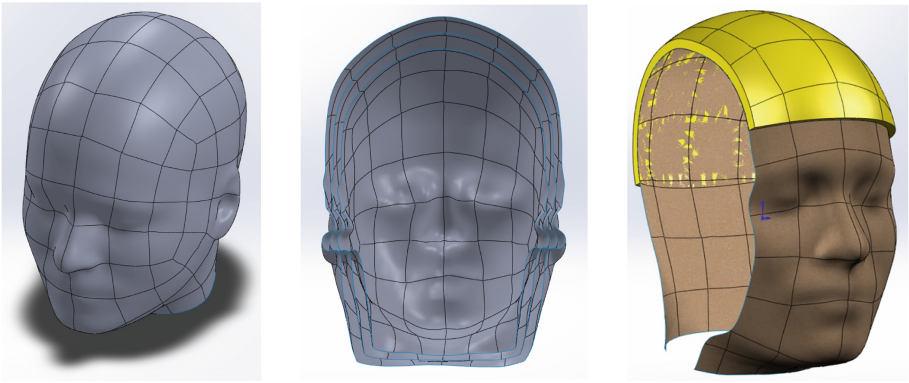

Fig. 4. Example body shapes (manikins) generated by our method and imported into SolidWork though our AddIn. Left: the average manikin of the MRI head model. Middle: cut-away of three manikins of this model with varying head/bi-tragion width (P5-50-95). Right: cutaway of the average manikin together with a perfectly fitting solid body obtained from the manikin by the SolidWorks features 'Intersect' and 'Shell'.

4 Discussion

The results in this paper show that our methodology is able to convert triangle mesh SSMs to B-spline parametric body models for a variety of shapes, without sacrificing on accuracy, water-tightness, or anatomical correspondence. Our methodology has three input parameters: number of patches, control point grid size, and the Tikhonov

regularization factor. It was empirically determined that accurate models with a limited number of control points can be obtained by balancing the number of patches (here ranging from 90 to 200) with the number of control points per patch (ranging from 8×8 to 12×12). For the models considered in this paper, the Tikhonov regularization factor, used to regularize the B-spline fitting of the patches, could be kept constant at 0.01. A further analysis on the femur dataset demonstrated that the resulting models are not too sensitive to the regularization factor, i.e. the amount of smoothing and the fitting error remained acceptable for regularization factors differing several orders of magnitude: Fig. 4, τ ranging from 0.001 to 0.1 for the femur with a 12×12 grid size. Nevertheless, a too low value might lead to an ill conditioned system, especially when the number of control points far exceeds the number of vertices in the patch. Too high values can result in significant artifacts at the patch boundaries as can be seen from Fig. 4.

The resulting SSMs are also easily imported in CAD software, via our AddIn, and can be used to generate a variety of body shapes that are sufficiently detailed for the ergonomic design of products. Using standard CAD-operations, available in SolidWorks, products or product parts can be constructed directly from the manikins to nicely conform to the contours of the human body, as demonstrated in Fig. 4. It should be noted, however, that certain CAD operations, like surface offsetting, are notoriously complicated and are not always able to generate valid results for organic shapes. We anticipate that the robustness of these algorithms will keep on improving, but also acknowledge that it might also help if our models would be smooth at patch boundaries (on top of the water-tightness we currently provide).

For future work, we envisage two main directions. On the one hand, we would like to further improve the B-spline approximation by (a) integrating the splitting of the mean mesh in patches with the quad-remeshing step for improved stability and (b) by including the boundary curve normals in the patch fitting for improved smoothness at the patch boundaries. On the other hand, we would like to further improve the modeling step by investigating the use of weighted PCA to compensate for patch size variations in the SSM and to extensively evaluate the derived B-spline SSMs in terms of model compactness, generalization ability, and specificity.

Acknowledgments. This work was financially supported by VLAIO grants TETRA-130771 and SB-141520.

References

1. Pheasant, S., Haslegrave, C.M.: Bodyspace: Anthropometry, Ergonomics and the Design of Work. CRC Press, Boca Raton (2016)
2. Motti, V.G., Caine, K.: Human factors considerations in the design of wearable devices. In: Proceedings of the Human Factors and Ergonomics Society Annual Meeting, vol. 58, no. 1, pp. 1820–1824. SAGE Publications, Thousand Oaks (2014)
3. Baek, S.Y., Lee, K.: Parametric human body shape modeling framework for human-centered product design. Comput.-Aided Des. **44**(1), 56–67 (2012)

4. Heimann, T., Meinzer, H.P.: Statistical shape models for 3D medical image segmentation: a review. Med. Image Anal. **13**(4), 543–563 (2009)
5. Davies, R.H., Twining, C.J., Cootes, T.F., Taylor, C.J.: Building 3-D statistical shape models by direct optimization. IEEE Trans. Med. Imaging **29**(4), 961–981 (2010)
6. Huysmans, T., Sijbers, J., Verdonk, B.: Automatic construction of correspondences for tubular surfaces. IEEE Trans. Pattern Anal. Mach. Intell. **32**(4), 636–651 (2010)
7. Allen, B., Curless, B., Popović, Z.: The space of human body shapes: reconstruction and parameterization from range scans. ACM Trans. Graph. **22**(3), 587–594 (2003)
8. Anguelov, D., Srinivasan, P., Koller, D., Thrun, S., Rodgers, J., Davis, J.: SCAPE: shape completion and animation of people. ACM Trans. Graph. **24**(3), 408–416 (2005)
9. Hasler, N., Stoll, C., Sunkel, M., Rosenhahn, B., Seidel, H.P.: A statistical model of human pose and body shape. Comput. Graph. Forum **28**(2), 337–346 (2009)
10. Chen, Y., Liu, Z., Zhang, Z.: Tensor-based human body modeling. In: IEEE Conference on Computer Vision and Pattern Recognition (CVPR), pp. 105–112. IEEE (2013)
11. Park, B.K., Reed, M.P.: Parametric body shape model of standing children aged 3–11 years. Ergonomics **58**(10), 1714–1725 (2015)
12. Pishchulin, L., Wuhrer, S., Helten, T., Theobalt, C., Schiele, B.: Building statistical shape spaces for 3D human modeling. Pattern Recogn. **67**, 276–286 (2017)
13. Quan, W., Matuszewski, B., Shark, L., Ait-Boudaoud, D.: 3-D facial expression representation using B-spline statistical shape model. In: British Machine Vision Conference, Vision, Video and Graphics Workshop, 10–13 September 2007, Warwick (2007)
14. Hu, N., Cerviño, L., Segars, P., Lewis, J., Shan, J., Jiang, S., Wang, G.: A method for generating large datasets of organ geometries for radiotherapy treatment planning studies. Radiol. Oncol. **48**(4), 408–415 (2014)
15. Peng, W., Feng, Z., Xu, C., Su, Y.: Parametric T-spline face morphable model for detailed fitting in shape subspace. In: Proceedings of the IEEE Conference on Computer Vision and Pattern Recognition, pp. 6139–6147 (2017)
16. Campen, M.: Partitioning surfaces into quadrilateral patches: a survey. Comput. Graph. Forum **36**(8), 567–588 (2017)
17. Bommes, D., Zimmer, H., Kobbelt, L.: Mixed-integer quadrangulation. ACM Trans. Graph. **28**(3), 77:1–77:10 (2009)
18. Kimmel, R., Sethian, J.A.: Computing geodesic paths on manifolds. Proc. Natl. Acad. Sci. **95**(15), 8431–8435 (1998)
19. Floater, M.S.: Parametrization and smooth approximation of surface triangulations. Comput. Aided Geom. Des. **14**(3), 231–250 (1997)
20. Floater, M.S.: Mean value coordinates. Comput. Aided Geom. Des. **20**(1), 19–27 (2003)
21. Bartels, R.H., Beatty, J.C., Barsky, B.A.: An Introduction to Splines for Use in Computer Graphics and Geometric Modeling. Morgan Kaufmann, Burlington (1987)
22. Li, X.S.: An overview of SuperLU: algorithms, implementation, and user interface. ACM Trans. Math. Softw. **31**(3), 302–325 (2005)
23. Capetillo-Cunliffe, L.: Loni: Laboratory of Neuro Imaging (2007)
24. Robinette, K.M., Daanen, H., Paquet, E.: The CAESAR project: a 3-D surface anthropometry survey. In: Second IEEE International Conference on 3-D Digital Imaging and Modeling, pp. 380–386 (1999)
25. Danckaers, F., Huysmans, T., Lacko, D., Ledda, A., Verwulgen, S., Van Dongen, S., Sijbers, J.: Correspondence preserving elastic surface registration with shape model prior. In: 22nd International Conference on Pattern Recognition (ICPR), pp. 2143–2148. IEEE (2014)